Supplementary Information for

"Diverse response of surface ozone to COVID-19 lockdown in China"

Yiming Liu[a,*#], Tao Wang[a,*], Trissevgeni Stavrakou[b], Nellie Elguindi[c], Thierno Doumbia[c], Claire Granier[c,d], Idir Bouarar[e], Benjamin Gaubert[f], Guy P. Brasseur[a,e,f]

[a]Department of Civil and Environmental Engineering, The Hong Kong Polytechnic University, Hong Kong, China;

[b]Royal Belgian Institute for Space Aeronomy, Brussels, Belgium;

[c]Laboratoire d'Aérologie, Toulouse, France;

[d]NOAA Chemical Sciences Laboratory and CIRES/University of Colorado, Boulder, CO, USA;

[e]Environmental Modeling Group, Max Planck Institute for Meteorology, Hamburg, Germany;

[f]Atmospheric Chemistry Observations and Modeling Laboratory, National Center for Atmospheric Research, Boulder, CO, USA;

*Correspondence to: Tao Wang (cetwang@polyu.edu.hk) and Yiming Liu (liuym88@mail.sysu.edu.cn)

[#]Now in School of Atmospheric Sciences, Sun Yat-sen University, Zhuhai, China

This file includes Supplementary text, and Supplementary Figures S1-S5, Supplementary Table S1-S2.

Supplementary text

Estimation of anthropogenic emissions in 2020

We estimated the anthropogenic emission for China in 2020 based on the MEIC 2017 (http://www.meicmodel.org) according to the control plan established by the Chinese government and the emission trends in recents years. From 2013 to 2017, the Chinese government launched the to Air Pollution Prevention and Control Action Plan to mitigate haze events. Zheng et al. (2018) compiled the trends of anthropogenic emissions during this period and demonstrated that the SO_2, NO_x, and PM (particulate matter, including PM_{10}, $PM_{2.5}$, and its components) emissions have been reduced significantly. In 2018, the Chinese government issued a Three-Year Action Plan (2018–2020) to further reduce the SO_2, NO_x, and PM emissions (http://www.gov.cn/zhengce/content/2018-07/03/content_5303158.htm). Previous control measures were implemented and the emissions were thought to continue decreasing after 2017. As the most recent available data on China's anthropogenic emissions are from 2017, we estimated the emissions for 2020 based on the MEIC 2017 according to the trends of these emissions in recent years (Zheng et al., 2018). Table S1 shows the scaling factors from 2017 to 2020 for NO_2, PM, and SO_2 in the power plant, industry, transportation, and residential sectors. The VOC emission was assumed to be unchanged from 2017 to 2020 because it increased by only 2% from 2013 to 2017 (Zheng et al., 2018). The NO_2, PM, and SO_2 emissions from transportation were also assumed constant from 2017 to 2020, considering that they had changed little during 2015–2017. The NO_x emission in the residential and industrial sectors was assumed to be the same in 2020 as in 2017 in view of its flat trend in recent years. Because the NO_x emission from power plants decreased by ~47% from 2013 to 2017 (11.7% per year), we assumed it to further decrease by 35% from 2017 to 2020. The same approaches were applied to the reductions of the PM and SO_2 emissions from 2017 to 2020. With these adjustments, we derived an estimated anthropogenic emission inventory for China in 2020. The model-simulated pollutant concentrations using this inventory showed a reasonable agreement with the surface measurement data during the period before the COVID-19 lockdown (Table S2, also see the Model evaluation section below), which suggested the estimated emission inventory was reasonable.

Estimated reduction of anthropogenic emissions during the CLD period

We estimated the emission reductions during the COVID-19 lockdown period according to the recent literature (Doumbia et al., 2021; Wang et al., 2020; Huang et al., 2020). For the transportation sector, the decrease in national traffic volume was estimated at 70% during the lockdown according to transportation index data. The industry emissions were assumed to decrease by 40% across China. The emissions of power plants were estimated to decrease by 30% due to the less consumption of electricity. The emissions of residential activities were assumed to increase by 10% due to more coal combustion and cooking. We kept the emissions from agriculture unchanged because they were less affected by the city lockdowns. Fig. 8 presents the reductions of NO_x, VOCs, CO, PM, and SO_2 emissions due to the changes in anthropogenic activities during the lockdown, which generally match the estimation by Huang et al. (2020). The observed pollutant concentrations during the lockdown period could faithfully captured by the CMAQ model using this estimated reduced emissions (Table S2, also see the Model evaluation section below), which suggested the estimated reductions of anthropogenic emissions were acceptable.

Model evaluation

Statistical parameters were calculated to validate the model performance in simulating the air pollutant concentrations from January 2 to February 12, 2020, including the mean observation (OBS), mean simulation (SIM), mean bias (MB), mean absolute gross error (MAGE), root mean square error (RMSE), index of agreement (IOA), and correlation coefficient (r). The equations of these statistical parameters can be found in Fan et al. (2013).

Table S2 shows the evaluation results of the simulated concentrations of SO_2, NO_2, CO, O_3 and $PM_{2.5}$ in China

for the periods before and during the COVID-19 lockdown, respectively. As the measured NO_2 by the catalytic conversion method in the national network overestimates the NO_2 (Xu et al., 2013), we adjusted the observed NO_2 data following the method proposed by Zhang et al. (2017) and Fu et al. (2019). Generally, the CMAQ model faithfully reproduced the observed concentrations of NO_2, SO_2, CO, $PM_{2.5}$ and O_3 with low biases during both peirods. The evaluation results suggested reasonable estimations of the anthropogenic emissions for the year 2020 and during the lockdown.

As we focused on the O_3 changes in NC, CC, and SC regions, we futher evaluated the modeling performace in simulating the variations of O_3 and NO_2 for these regions. Fig. S1 shows the time series of simulated and observed O_3 and NO_2 mixing ratios. The magnitude and variation of the observed NO_2 mixing ratios for these three regions were all well captured by the CMAQ model. The observed O_3 mixing ratios for three regions were also reasonably reproduced. Both the simulation and observation showed an O_3 increase in NC and CC but a decrease in SC (also shown in Fig. 4). However, the O_3 mixing ratio in NC during the lockdown was underestimated, probably due to the uncertainties in meteorological simulation. The O_3 mixing ratio in SC was generally overestimated during the simulation period, which might be attributed to the influence of the overestimated O_3 concentrations on the ocean. Nevertheless, the model was able to faithfully capture the observed O_3 variations in these three regions.

Overall, despite some uncertainties, the CMAQ model performance is acceptable and can support further analysis of O_3 changes during the COVID-19 city lockdowns.

Reference:

Doumbia, T., Granier, C., Elguindi, N., Bouarar, I., Darras, S., Brasseur, G., Gaubert, B., Liu, Y., Shi, X., Stavrakou, T., Tilmes, S., Lacey, F., Deroubaix, A., and Wang, T. Changes in global air pollutant emissions during the COVID-19 pandemic: a dataset for atmospheric chemistry modeling. Earth Syst. Sci. Data Discuss, 2021. (In review).

Fan, Q., Liu, Y. M., Wang, X. M., Fan, S. J., Chan, P. W., Lan, J., and Feng, Y. R.: Effect of different meteorological fields on the regional air quality modelling over Pearl River Delta, China, Int. J. Environ. Pollut., 53, 3-23, 10.1504/ijep.2013.058816, 2013.

Fu, X., Wang, T., Zhang, L., Li, Q., Wang, Z., Xia, M., Yun, H., Wang, W., Yu, C., Yue, D., Zhou, Y., Zheng, J., and Han, R.: The significant contribution of HONO to secondary pollutants during a severe winter pollution event in southern China, Atmos. Chem. Phys., 19, 1-14, 10.5194/acp-19-1-2019, 2019.

Huang, X., Ding, A., Gao, J., Zheng, B., Zhou, D., Qi, X., Tang, R., Wang, J., Ren, C., Nie, W., Chi, X., Xu, Z., Chen, L., Li, Y., Che, F., Pang, N., Wang, H., Tong, D., Qin, W., Cheng, W., Liu, W., Fu, Q., Liu, B., Chai, F., Davis, S. J., Zhang, Q., and He, K.: Enhanced secondary pollution offset reduction of primary emissions during COVID-19 lockdown in China, National Science Review, 10.1093/nsr/nwaa137, 2020.

Wang, P., Chen, K., Zhu, S., Wang, P., and Zhang, H.: Severe air pollution events not avoided by reduced anthropogenic activities during COVID-19 outbreak, Resources, Conservation and Recycling, 158, 104814, https://doi.org/10.1016/j.resconrec.2020.104814, 2020.

Xu, Z., Wang, T., Xue, L. K., Louie, P. K. K., Luk, C. W. Y., Gao, J., Wang, S. L., Chai, F. H., and Wang, W. X.: Evaluating the uncertainties of thermal catalytic conversion in measuring atmospheric nitrogen dioxide at four differently polluted sites in China, Atmos. Environ., 76, 221–226, https://doi.org/10.1016/j.atmosenv.2012.09.043, 2013.

Zhang, L., Li, Q. Y., Wang, T., Ahmadov, R., Zhang, Q., Li, M., and Lv, M. Y.: Combined impacts of nitrous acid and nitryl chloride on lower-tropospheric ozone: new module development in WRF-Chem and application to China, Atmos Chem Phys, 17, 9733-9750, 10.5194/acp-17-9733-2017, 2017.

Zheng, B., Tong, D., Li, M., Liu, F., Hong, C., Geng, G., Li, H., Li, X., Peng, L., Qi, J., Yan, L., Zhang, Y., Zhao, H., Zheng, Y., He, K., and Zhang, Q.: Trends in China's anthropogenic emissions since 2010 as the consequence of clean air actions, Atmos. Chem. Phys., 18, 14095-14111, 10.5194/acp-18-14095-2018, 2018.

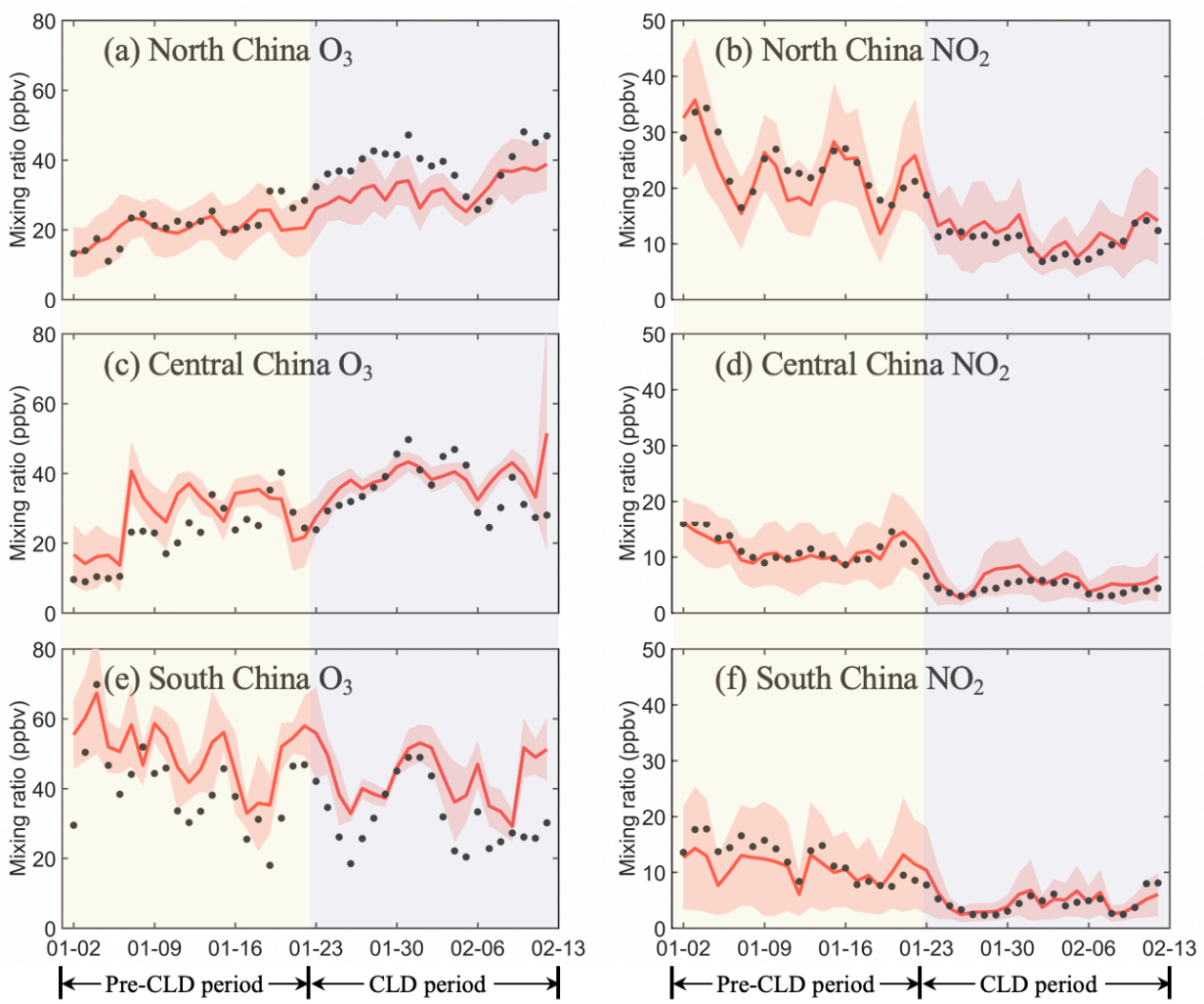

Figure S1: Time series of observed (black points) and simulated (red lines) mixing ratios of maximum daily average 8-h (MDA8) O_3 and NO_2 in North China, Central China, and South China from 2 January to 12 February 2020. The solid lines are the simulated average value and the shaded areas mark the standard deviations. The observed NO_2 data were adjusted based on the method proposed by Zhang et al. (2017) and Fu et al. (2019): $NO_{2\,OBS} = NO'_{2\,OBS} \times \frac{NO_{2\,SIM}}{NO_{2\,SIM}+NO_{z\,SIM}+NO_{3\,SIM}^{-}}$, where $NO'_{2\,OBS}$ is the measured NO_2 data by the catalytic conversion technique, $NO_{2\,SIM}$, $NO_{z\,SIM}$, and $NO_{3\,SIM}^{-}$ are the simulated data of NO_2, NO_z, and particulate nitrate, respectively, using the WRF-CMAQ model.

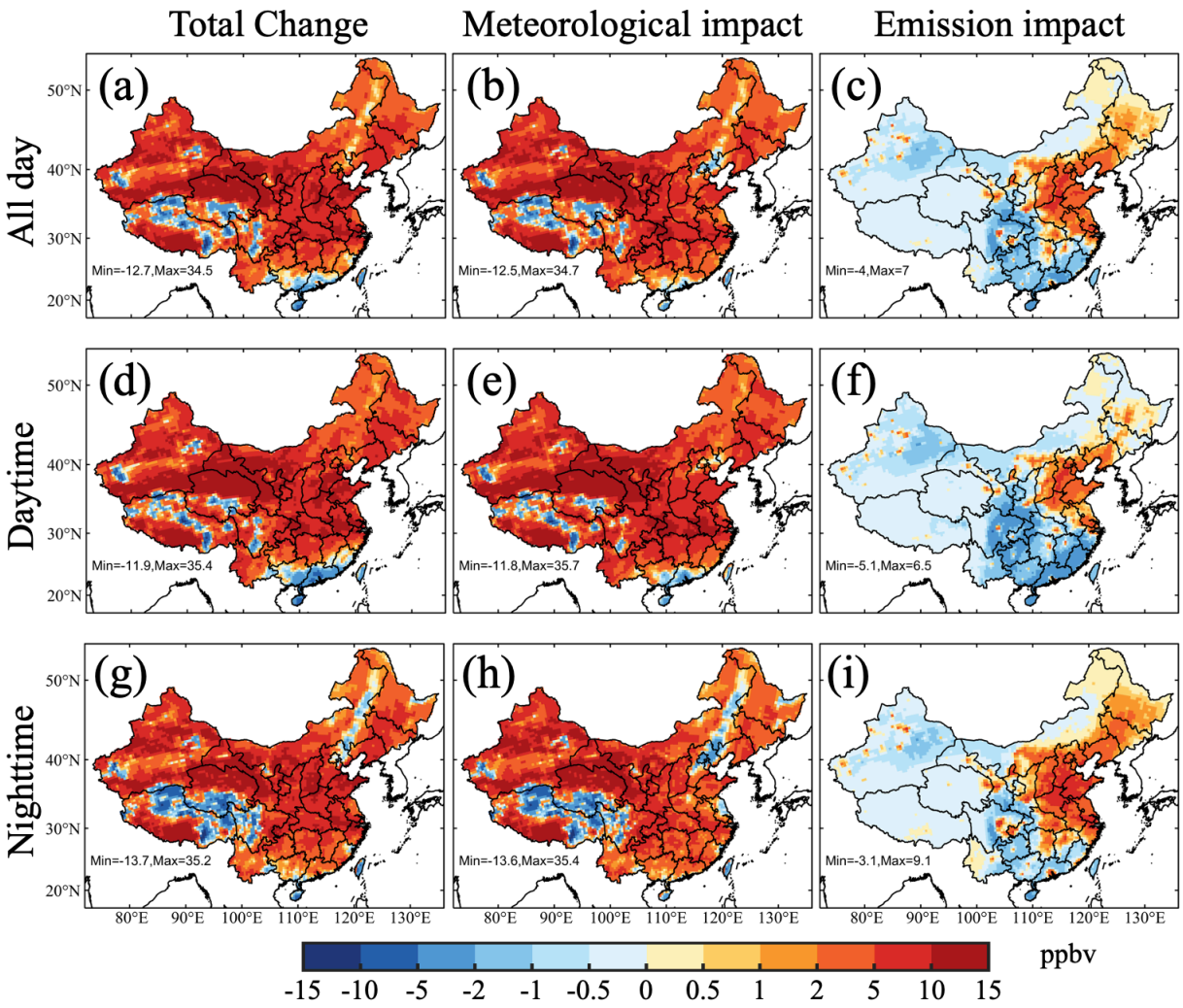

Fig. S2: Simulated changes in O_3 mixing ratios across China during the COVID-19 lockdown period and contributions from meteorological changes and emission reductions. (a, d, g) The simulated total O_3 changes for all-day average, daytime average, and nighttime average during the CLD period relative to the pre-CLD period. (b, e, h) Contribution of meteorological changes to O_3 for all-day average, daytime average, and nighttime average. (c, f, i) The same with (b, e, h), respectively, but for contribution of emission reductions.

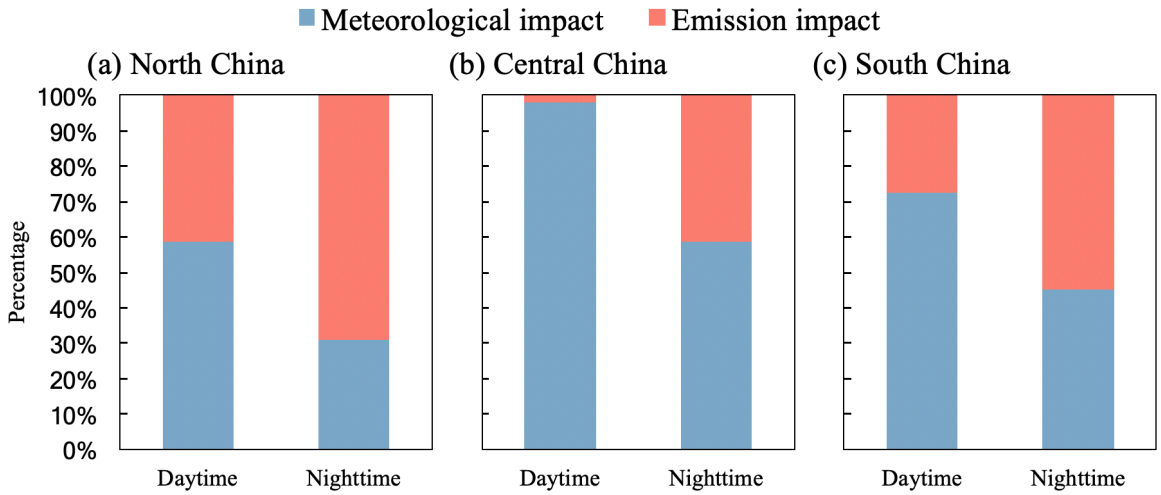

Figure S3 The contributions of meteorological changes and emission reduction to the changes in daytime and nighttime O_3 concentrations during the CLD period compared with the pre-CLD period. (a) North China; (b) Central China; (c) South China

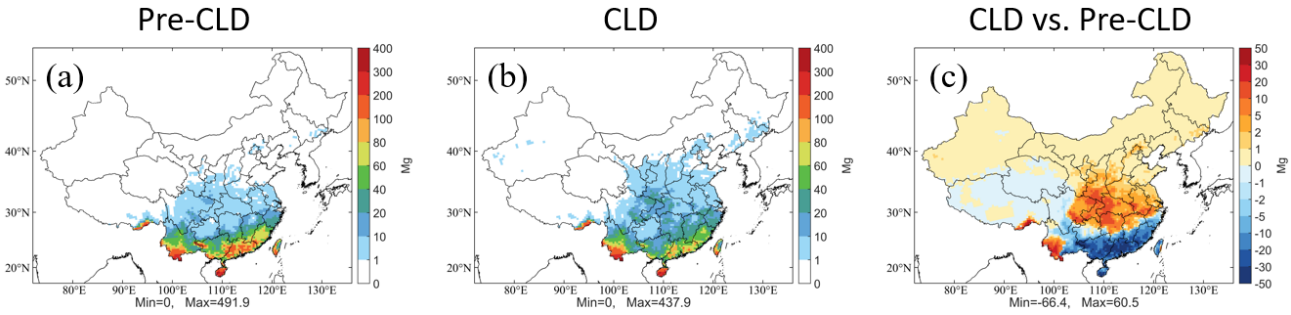

Figure S4: Biogenic isoprene emissions during the pre-CLD and CLD periods and their difference (CLD minus pre-CLD).

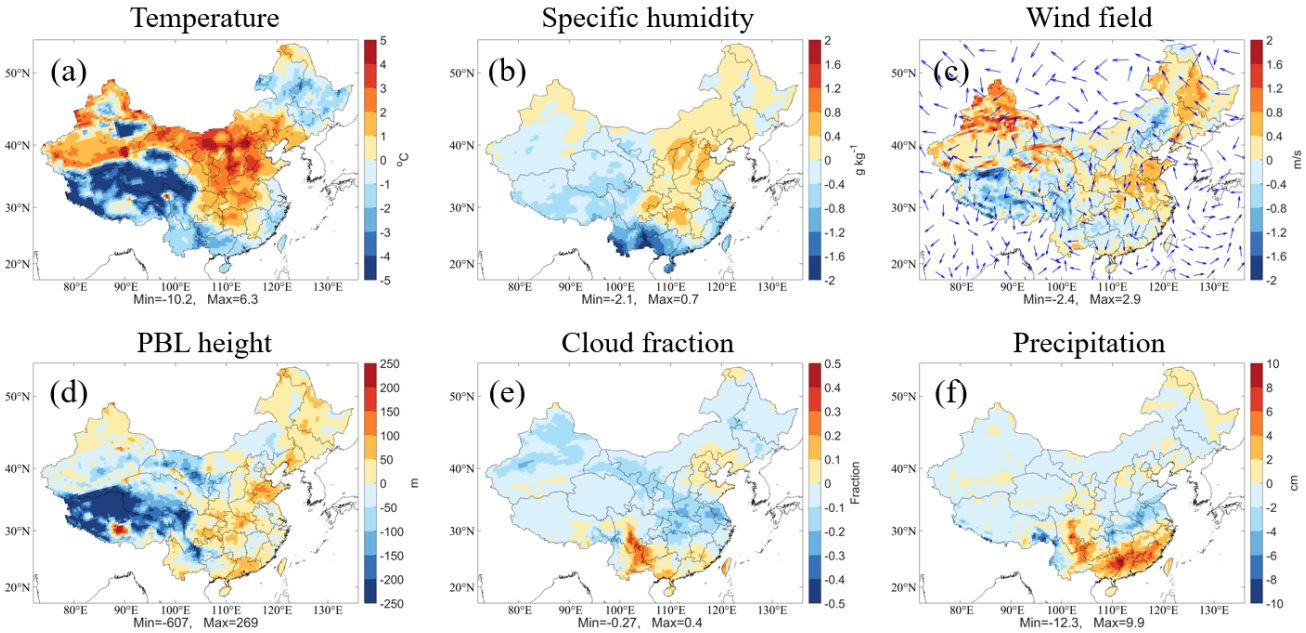

Figure S5: Model simulated changes in nighttime temperature at 2 m height, specific humidity at 2 m height, wind field at 10 m height, planetary boundary layer (PBL) height, cloud fraction, and precipitation during CLD period relative to pre-CLD period. In panel (c), the shaded color and vector represent the wind speed and wind direction, respectively.

Table S1: Scaling factors applied to different economic sectors in order to estimate the anthropogenic emissions of China for the year 2020 based on the 2017 MEIC emission inventory.

Emitted species	Power plants	Industry	Residence	Transportation
NO_x	-35%	-	-	-
SO_2	-40%	-40%	-25%	-
PM	-	-20%	-30%	-

Table S2: Evaluation results of the air pollutants across China for the pre-CLD (2-22 January 2020) and CLD (23 January-12 February 2020) periods. OBS is mean observation; SIM is mean simulation; MB is mean bias; MAGE is mean absolute gross error; RMSE is root mean square error; IOA is index of agreement; *r* is correlation coefficient; OBS, SIM, MB, MAGE, and RMSE have the same units as given in the first column, while IOA and *r* have no unit.

Species	Period	OBS	SIM	MB	MAGE	RMSE	IOA	*r*
SO_2 (ppbv)	Pre-CLD	4.9	5.4	0.5	3.8	4.5	0.79	0.35
	CLD	4.1	4.1	0.0	3.1	3.8	0.77	0.33
NO_2[a] (ppbv)	Pre-CLD	14.7	12.5	-2.2	5.1	6.0	0.90	0.49
	CLD	6.6	6.7	0.1	3.1	3.7	0.89	0.58
CO (ppmv)	Pre-CLD	0.94	0.66	-0.28	0.42	0.48	0.88	0.40
	CLD	0.75	0.51	-0.24	0.34	0.40	0.88	0.40
MDA8 O_3 (ppbv)	Pre-CLD	26.2	30.1	3.9	10.5	13.0	0.94	0.35
	CLD	36.0	37.6	1.6	10.5	12.9	0.97	0.38
$PM_{2.5}$ (μg/m^3)	Pre-CLD	69.3	71.8	2.4	33.0	41.6	0.90	0.51
	CLD	55.3	52.7	-2.6	25.9	34.2	0.90	0.55

a The observed NO_2 data were adjusted based on the method proposed by Zhang et al. (2017) and Fu et al. (2019): $NO_{2\,OBS} = NO'_{2\,OBS} \times \frac{NO_{2\,SIM}}{NO_{2\,SIM}+NO_{z\,SIM}+NO^-_{3\,SIM}}$, where $NO'_{2\,OBS}$ is the measured NO_2 data by the catalytic conversion technique, $NO_{2\,SIM}$, $NO_{z\,SIM}$, and $NO^-_{3\,SIM}$ are the simulated data of NO_2, NO_z, and particulate nitrate, respectively, using the WRF-CMAQ model.